International Journal of Hydrogen Energy 219 (2026) 154020

Contents lists available at ScienceDirect

International Journal of Hydrogen Energy

journal homepage: www.elsevier.com/locate/he

Simulation and analysis of methane thermal decomposition in an aerosol flow reactor

İzzet Karabay [a], İsmail Ekmekci [b,*]

[a] EHSiM Elektronik Harp Sist. Müh. Ticaret A. Ş., ELD Director, Hacettepe Teknokent, 06800, Ankara, Türkiye
[b] İstanbul Ticaret Üniversiti, Engineering Faculty, 34840, İstanbul, Türkiye

ARTICLE INFO

Keywords:
Methane decomposition
Aeresol flow reactor
Methane pyrolysis
Hydrogen production
CO_2-Free
Reaction engineering
Catalysis flow reaction
CFD modelling

ABSTRACT

The thermal decomposition of methane represents a significant pathway for producing high-purity hydrogen. Aerosol flow reactors, particularly when coupled with concentrated solar energy, are considered highly suitable for this thermochemical process. This study presents a comprehensive Computational Fluid Dynamics (CFD) model of methane decomposition within an aerosol flow reactor. The model integrates coupled phenomena, including gas flow dynamics, chemical reaction mechanisms, radiative and convective heat transfer, and a discrete phase model for carbon particles. The development of a generalized, predictive model is crucial for reactor optimization, and CFD modeling offers rapid prediction capabilities. Consequently, this work validates a novel CFD model against previously published experimental and theoretical data from an Aerosol Quartz Flow Reactor (AFR). The model computes methane decomposition rates and the spatial dispersion of components (H_2, C, CH_4) under various feeding rates and temperature profiles.

1. Introduction

Hydrogen is increasingly recognized as a cornerstone of future energy systems due to its high energy density, clean combustion profile, and versatility in both stationary and mobile applications. Among the various production pathways, methane decomposition has attracted significant attention because methane possesses the highest hydrogen density of all gaseous fuels. In addition to hydrogen, the process yields solid carbon, which can be obtained in pure form and utilized in industrial applications such as pigments, reinforcing agents, and advanced carbon materials. Unlike conventional reforming methods that require additional reactants such as steam or carbon dioxide, methane decomposition is a direct process involving only methane, thereby simplifying the reaction mechanism and facilitating high-purity hydrogen production.

The integration of solar energy into methane decomposition processes offers a promising route for sustainable hydrogen generation. Thermochemical conversion enables the direct storage of solar energy in chemical bonds, thereby coupling renewable energy utilization with hydrogen production. Aerosol reactors, in particular, have emerged as strong candidates for solar-driven methane decomposition because they allow direct absorption of concentrated solar radiation by both the gas phase and suspended carbon particles. This design leads to high heat transfer rates and efficient reaction kinetics, while the quartz tubular configuration ensures durability and optical transparency.

The aim of our study is to investigate the methane decomposition reaction process, emphasizing heat and mass transfer events; to evaluate the aerosol reactor concept for high-temperature decomposition; to assess the applicability of these tube reactors in methane decomposition; to identify critical parameters affecting reactor performance, including radiation-convection heat transfer mechanisms and chemical conversion kinetics; and to contribute, particularly regarding the suitability of these reactors for large-scale hydrogen production.

While previous CFD studies of methane pyrolysis have advanced understanding of reactor thermodynamics and kinetics, they generally lack the ability to simultaneously resolve radiative transfer, multiphase transport, and carbon particle evolution. Such simplifications limit predictive accuracy under solar driven conditions, where radiation–particle interactions strongly influence reactor performance. The present study introduces a CFD framework that explicitly couples radiative heat transfer, heterogeneous reaction pathways, and dynamic carbon particle behavior. This integrated approach enables more

This article is part of a special issue entitled: IHTEC-2025 (Colpan) published in International Journal of Hydrogen Energy.

* Corresponding author.
E-mail address: iekmekci@ticaret.edu.tr (İ. Ekmekci).

https://doi.org/10.1016/j.ijhydene.2026.154020
Received 19 November 2025; Received in revised form 28 January 2026; Accepted 11 February 2026
Available online 18 February 2026
0360-3199/© 2026 Hydrogen Energy Publications LLC. Published by Elsevier Ltd. All rights are reserved, including those for text and data mining, AI training, and similar technologies.

realistic simulation of solar driven methane pyrolysis and provides new insights into reactor design and optimization beyond the capabilities of existing models.

2. Literature review

Extensive research has been conducted to understand methane decomposition mechanisms, catalyst stability, and reactor performance. Snoeck investigated Ni catalysts both experimentally and theoretically, highlighting kinetic aspects of methane decomposition [3]. These studies underscore the importance of catalyst stability and activity in sustaining long-term hydrogen production.

Such modeling approaches are crucial for predicting reactor performance and optimizing design. Matowich conducted experimental studies on methane decomposition in aerosol reactors [5], while Wiemer and co-workers extended this work by integrating concentrated solar energy, developing mathematical models to explain kinetic parameters, and testing solar reactor prototypes [1,2].

Deutschmann applied computational fluid dynamics (CFD) to partial methane oxidation, developing two- and three-dimensional models relevant to decomposition processes [4].

Hirsch examined solar hydrogen production using a 5 kW vortex-flow reactor, reporting a maximum methane conversion of 67% at 1600 K and 1 bar [6].

Trommer investigated kinetic mechanisms of thermal decomposition via direct irradiation of carbon-laden vortex flows, reporting activation energies between 147 and 162 kJ/mol and frequency factors in the range of 1.07×10^6–7.54×10^6 s^{-1} [7].

Stephane designed and tested a high-temperature solar chemical reactor, performing both theoretical and experimental evaluations of methane splitting [8].

Mianowski, A. et al. have conducted a detailed literature review examining the state of knowledge on methane pyrolysis, examining whether the process can be considered an elementary reaction, and determining the extent to which thermodynamic and kinetic models reflect micro- and macroscale behavior. This study bridges the gap between phenomenological thermodynamics and kinetic modeling, emphasizing that methane pyrolysis cannot be fully represented by a single, universal model. Furthermore, they identified research gaps in the link between micro-scale radical mechanisms and macro-scale reactor performance [9].

In their review, Moghaddam, AL. et al. emphasize that methane pyrolysis is a critical methodology for "turquoise hydrogen," but they emphasize that integrated models integrating radical chemistry, catalyst transformations, and reactor-scale engineering analyses are still lacking in this field. They note that the integration of microscale radical mechanisms with macroscale reactor performance is not yet complete [10].

While these studies provide valuable insights, most existing CFD models of aerosol reactors remain limited in scope. One dimensional energy balance models, although computationally efficient, cannot resolve radial temperature gradients, localized hot spots, or particle migration across the reactor cross section. Many prior models also neglect thermophoretic forces, which are critical for predicting particle drift and deposition patterns in high temperature flows. Furthermore, radiation is often treated simplistically, with uniform absorption assumptions that ignore wavelength dependence and scattering effects. These simplifications restrict predictive accuracy, particularly under solar driven conditions where radiative transfer dominates heat transport. In addition, earlier models rarely integrate multiphase particle tracking with radiation transport, limiting their ability to capture the coupled dynamics of gas flow, particle motion, and radiative heating.

In contrast, the present study employs a two dimensional Discrete Phase Model (DPM) coupled with the Discrete Ordinates (DO) radiation method, which overcomes these deficiencies. The 2D framework resolves both axial and radial gradients, enabling accurate prediction of temperature fields and conversion zones. The DPM explicitly tracks particle trajectories, incorporating drag, lift, and thermophoretic forces, thereby reproducing experimentally observed ring-shaped particle concentrations. The DO radiation model accounts for absorption, emission, and scattering of carbon particles, with wavelength dependent optical properties, ensuring realistic representation of radiative heat transfer. By solving radiation, convection, chemical kinetics, and particle dynamics simultaneously, this integrated approach provides a more comprehensive and predictive description of aerosol reactor physics than prior 1D or simplified CFD models.

Previous CFD studies of aerosol reactors have provided valuable insights, but most rely on one dimensional approximations that cannot resolve radial temperature gradients or particle migration. Such simplifications neglect thermophoretic forces and often treat radiation as uniform absorption. These limitations restrict predictive accuracy under solar driven conditions. In contrast, the present study employs a two dimensional Discrete Phase Model (DPM) coupled with the Discrete Ordinates (DO) radiation method, enabling resolution of radial gradients, incorporation of thermophoretic effects, and explicit modeling of radiation–particle interactions. This integrated framework provides a more realistic representation of aerosol reactor physics than prior 1D or simplified CFD approaches.

The efficiency of methane decomposition is governed by coupled heat and mass transfer phenomena. Radiation and convection are the primary modes of heat transfer, while chemical conversion kinetics determine the rate and extent of hydrogen formation. These aspects are particularly critical in solar-driven systems, where concentrated radiation must be effectively absorbed and converted into chemical energy.

Several solar-assisted methods have been explored for hydrogen production and solar energy storage, including steam reforming, CO_2 reforming, and hydrocarbon cracking. Among these, the aerosol reactor has emerged as a strong candidate for methane decomposition. Its quartz tubular design enables direct absorption of solar radiation by both the gas phase and suspended carbon particles, resulting in high heat transfer rates. The process yields hydrogen of high purity, with relatively straightforward purification requirements, making quartz-based aerosol reactors a rational choice for solar-driven methane splitting.

Building on these insights and addressing the identified limitations, the present study develops a two dimensional CFD framework that integrates chemical kinetics, multiphase particle dynamics, and radiative heat transfer, as detailed in following section.

3. Approach and methodology

This study is primarily focused on the development of.a comprehensive understanding of the methane decomposition mechanism by examining the influence of several critical parameters, including chemical reaction kinetics, radiation heat transfer, and multiphase flow involving discrete particles. The analysis focuses on a two-dimensional reactor configuration to demonstrate how these parameters interact and affect system performance.

Previous investigations, such as those conducted by Dahl [1], employed one-dimensional energy balance equations to provide preliminary insights. While such approaches offer rapid guidance for engineers, they do not adequately capture the spatial distribution of parameters across the reactor cross-section. For design engineers, this distribution is essential to evaluate localized effects and ensure reliable reactor operation. Moreover, maintaining mathematical consistency in solution data presents a significant challenge when multiple coupled phenomena are considered simultaneously. To address these difficulties, finite element methods are adopted, as they enable the simultaneous resolution of numerous parameters and facilitate the generation of mathematically integrated solutions.

Hydrogen production using solar energy in aerosol reactors represents an attractive pathway due to its simplicity, direct utilization of solar radiation, and ease of processing. In this context, methane

decomposition within aerosol reactors is characterized as a heterogeneous chemical reaction. The reacting fluid flow involves complex interactions among gas-phase chemistry, discrete particle motion, and radiation transport. Recent progress in computational resources the refinement of advanced computational algorithms and the accessibility. of detailed elementary reaction mechanisms have significantly enhanced the ability to model such systems. Nevertheless, the governing equations remain highly stiff because of the wide range of time scales introduced by chemical kinetics.

To reduce computational complexity, slightly simplified models are often used in simulations. However, these simplifying assumptions can present problems in situations where there are strong interactions between flow dynamics, discrete phase behavior, radiation transfer, and chemical reactions. When excessive simplifications are made, the accuracy and reliability of the results may be insufficient. To overcome these problems with simplifying assumptions, the simulations in our study were designed to include more detailed chemical reaction mechanisms. Furthermore, simulations were performed using FLUENT, a commercial computational fluid dynamics (CFD) software, combined with developed external subroutines [19]. This integrated approach allows for a more rigorous representation of the methane decomposition process, capturing the complex interplay of physical and chemical phenomena within the reactor environment.

4. Methane decomposition

Extensive and detailed researches have been conducted to understand the reaction mechanisms underlying the thermal dissociation of hydrocarbons, particularly natural gas, propane, ethylene, and methane. Among these studies, hydrogen production from methane (CH_4) has attracted considerable attention due to its great potential. Steinberg has extensively investigated the thermal decomposition of methane for hydrogen production and is considered one of the leading researchers in this field [12]. The fundamental chemical methodology here is the decomposition of methane into hydrogen (H_2) and solid carbon (C) in the form of carbon black. Methane (CH_4) decomposes into carbon (C) black and hydrogen according to the following chemical reactions at different temperatures:

$$CH_4 \rightarrow C + 2H_2 \ \Delta H_{298\ K} = 74.9\ \text{kJ/mol} \quad (1a)$$

$$CH_4 \rightarrow C + 2H_2 \ \Delta H_{1000\ K} = 89{,}8\ \text{kJ/gmol} \quad (1b)$$

Methane cracking is an endothermic process that requires elevated temperatures[16]. According to thermodynamic principles, methane begins to decompose into solid carbon and hydrogen gas once the temperature exceeds 300 °C, even in the absence of a catalyst[17]. In practice, however, achieving significant conversion without a catalyst is difficult below 1200 °C, due to kinetic limitations and the high activation energy needed to break the strong C–H bonds in methane [21]. Reported activation energies for non-catalytic methane decomposition vary across studies: Rodat et al. [22] measured 370 kJ/mol, while Keipi et al. [23] reported 422 kJ/mol. Other authors have placed the values within the range of 356–452 kJ/mol [24–27].

For non-catalytic thermal decomposition at high temperatures (typically >1200 °C), the reaction is generally accepted to be first-order in methane concentration. This is supported by numerous fundamental studies using shock tubes, flow reactors, and modeling work where the rate law is expressed as:

$$r = k\cdot[CH_4] \quad (2a)$$

where r is the reaction rate and k is the rate constant following the Arrhenius equation. Our model the reaction using Arrhenius-based, finite-rate chemistry. Although the reaction order is not explicitly stated in the studies, their use of a single-reactant, basic reaction mechanism (CH_4 → products) implies a first-order reaction. The rate expression typically used in our CFD models is as follows:

$$R_{CH_4} = A \exp\left(-E_a / RT\right)[CH_4]^n \quad (2b)$$

where $n = 1$ for first-order kinetics.

Muradov [13,14] and Kim [11] in catalytic decomposition over carbon materials often apply first-order or Langmuir-Hinshelwood models that simplify to first-order at low methane pressures. Trommer et al. [7] and Rodat et al. [22] who studied solar-driven decomposition, also used first-order global kinetics for modeling. For the specific numerical study presented in the manuscript, the methane cracking reaction is effectively treated as first-order with respect to methane concentration[18]. This is the standard approach in CFD models of tubular aerosol/reactor systems for simplifying computations while retaining accuracy.

The earliest theoretical and experimental investigations of methane decomposition were carried out by Cantelo in 1927. His work established that the onset of decomposition occurs at approximately 400 °C, with complete decomposition achieved at 1500 °C [20]. Subsequent studies have refined the understanding of kinetic parameters. For example, Holmen reported an activation energy of 370 kJ/mol within the temperature range of 1770K–2270K [11]. Tessner determined that the activation energy required for the nucleation of carbon particles during methane decomposition (316.8 kJ/mol) exceeds that associated with the growth of carbon crystallites [22]. Shock tube reactor studies have further reported activation energies in the range of 356–402 kJ/mol at temperatures between 2000K–3000K. Steinberg, in contrast, reported a significantly lower activation energy of 131 kJ/mol under conditions of 973–1173K and pressures of 28–56atm [1].

Previous studies have reported a wide range of activation energies for methane decomposition, reflecting differences in reactor type, operating conditions, and catalyst morphology. Shock tube experiments at 2000K–3000K yielded values between 356 and 402 kJ/mol, while Holmen reported 370 kJ/mol in a cylindrical reactor at 1770K–2270K. In contrast, Steinberg observed a significantly lower value of 131 kJ/mol under high pressure tubular flow conditions (973K–1173K). More recent catalytic studies demonstrate that carbon surfaces substantially reduce the energy barrier. Muradov reported activation energies of 236 kJ/mol for black carbon catalysts (1023–1223 K) and 201 kJ/mol for activated carbon catalysts (873–1173 K), while Kim found similar values (~200 kJ/mol) for activated carbons. These results highlight that carbon acts as both a catalyst and a product, providing active sites that stabilize radical intermediates and facilitate decomposition.

In the present work, the activation energy range of 200–211 kJ/mol was obtained by regression fitting of experimental conversion data from Muradov, Kim, and related studies, ensuring consistency with carbon catalyzed pathways rather than purely thermal decomposition. A sensitivity analysis was performed by varying the activation energy ±10% around the fitted values. The results showed that methane conversion changed by less than 7% across the studied temperature range, confirming that the CFD predictions are robust to small variations in kinetic parameters. This analysis supports the reliability of the chosen activation energy range and its suitability for modeling carbon assisted methane decomposition in aerosol reactors.

In addition to thermal studies, considerable effort has been devoted to examining the role of catalysts in methane decomposition. Muradov and his collaborators have investigated carbon-based catalysis, developing a model that describes the influence of various carbon catalysts and dimensional parameters on methane decomposition within fluidized bed reactors, supported by experimental data [13,14]. Wiemer and colleagues have also contributed to this area, focusing on solar-driven processes. Dahl and co-workers studied methane decomposition in solar aerosol reactors, proposing a mathematical model to describe the reaction mechanism [1]. Their subsequent work explored the feasibility of aerosol reactors for pilot-scale applications [2].

Building upon these foundations, the present study develops a two-

dimensional numerical model to describe methane decomposition in an aerosol quartz reactor, similar to that employed by Matowich. The model integrates transport equations, energy balance, chemical kinetics, discrete phase flow, and radiative energy transfer, thereby providing a comprehensive representation of the process. By employing validated kinetic and process parameters, the model captures the complex transport phenomena and reaction mechanisms that govern methane decomposition in solar-driven aerosol reactors.

5. Reactor model

In the present study, an aerosol reactor was employed with dimensions identical to those used in the experiments conducted by Matowich, thereby enabling direct comparison and validation of results against prior work. The reactor has a total length of 0.914 m and an internal diameter of 0.076 m, as illustrated in Figs. 1 and 2. Methane was introduced at the top of the reactor at five different feed rates. To enhance the decomposition reaction, carbon particles were co-fed with methane. The dissociation rate of CH_4 was determined by measuring the thermal conductivity of the effluent gas after the removal of carbon black particles from the sample stream [1,2].

A radial flow of hydrogen (H_2) was maintained at a constant rate of 0.094 mol/s through a porous reaction tube. This configuration provided a protective fluid-wall that prevented carbon black deposition on the reactor walls. The carbon feed rate was fixed at 1.2 g/s for all operating conditions. The carbon particles had a surface area of 3.14×10^{-8} m^2 and an emissivity value of 0.93. The reactor wall temperature was varied between 1533 K and 2144 K across different experimental runs. The residence time of methane within the reactor was controlled by three parameters: the inlet methane flow rate, the radial hydrogen flow rate, and the reactor wall temperature. These operating conditions collectively governed the extent of methane decomposition and hydrogen production. The specific wall temperatures and methane feed rates applied in the experiments are summarized in Table_1 [5] (see Table 2).

6. Numerical methodology and computational framework

The numerical model developed in this study is based on computational fluid dynamics (CFD) solutions, designed to integrate the fundamental mechanisms of methane decomposition and to illustrate the spatial distribution of chemical conversion within the reactor in two dimensions. The aerosol reactor model used in this study is inherently a three-dimensional axially symmetric system. However, to balance computational efficiency with physical accuracy, a two-dimensional axially symmetric CFD model was chosen. The reactor geometry is cylindrical, and the boundary conditions (methane feed, radial hydrogen injection, wall heating) are symmetric around the central axis. Under these conditions, the dominant transport events—laminar flow, radiative heat transfer, and particle migration—are primarily governed by axial and radial gradients, which can be adequately represented in a 2D axially symmetric framework. This approach has been widely adopted in CFD studies of tubular reactors because it captures the fundamental physics while significantly reducing computational cost compared to full 3D simulations. However, the primary focus of this study is the combined dynamics of radiation, convection, and chemical kinetics dominated by axial and radial gradients.

Therefore, the 2-dimensional axially symmetric model provides a sufficiently accurate representation of reactor physics for the scope of this study.

Previous investigations in this field have primarily relied on experimental approaches or simplified one-dimensional numerical analyses, which limited the ability to capture the complex interactions occurring across the reactor cross-section.

To overcome these limitations, the present model incorporates the appropriate governing equations, including conservation of energy, mass, and momentum, as well as species transport equations. In addition, boundary conditions were defined to account for radiation heat transfer, molecular diffusion, and particulate motion, thereby ensuring a comprehensive representation of the physical and chemical processes within the aerosol reactor.

The decomposition of methane involves multiple coupled phenomena, including chemical reactions, mass transfer, heat transfer, discrete phase effects, thermophoresis, and particle lift forces (Fig. 2). Accurate definition of the chemical conversion mechanism is particularly critical, as it requires the integration of complex governing equations and presents significant modeling challenges.

The flow within the reactor is characterized as a two-phase system, consisting of continuous methane gas and dispersed solid carbon particles. Carbon particles are introduced at the reactor inlet together with methane, and additional particles are generated in situ as a result of the decomposition reaction. To capture these dynamics, a discrete phase flow model was employed to describe the transport and interaction of carbon particles, methane, and hydrogen gases along the reactor length.

Furthermore, thermophoretic forces and lift effects were incorporated into the numerical framework to account for particle migration and distribution within the flow field. These additions enhance the accuracy of the model by reflecting the physical phenomena that influence particle behavior during methane decomposition in solar-driven aerosol reactors.

The ANSYS_FLUENT commercial package was employed to execute the computational fluid dynamics (CFD) simulations presented in this study. This code is widely recognized and extensively validated, making it a reliable tool for the formulation and solution of fluid flow problems. Its versatility allows for the straightforward implementation of complex flow configurations and the integration of chemical reaction mechanisms into the computational framework.

The simulations were based on the fundamental conservation and balance equations that govern laminar finite-rate flow fields. Specifically, the governing equations employed are of the Navier–Stokes type, which describe the conservation of mass, momentum, and energy for laminar and mixed flow regimes.

The Reynolds number (Re) was calculated to verify the assumption of laminar flow in the aerosol reactor. The general expression is:

$$\mathrm{Re}=(\rho \cdot u \cdot D)/\mu \tag{3}$$

where:

ρ = gas density (kg/m^3)

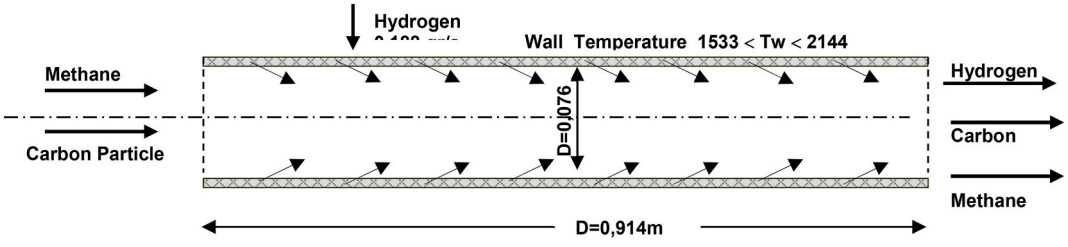


Fig. 1. Schematic representation of aerosol flow reactor.

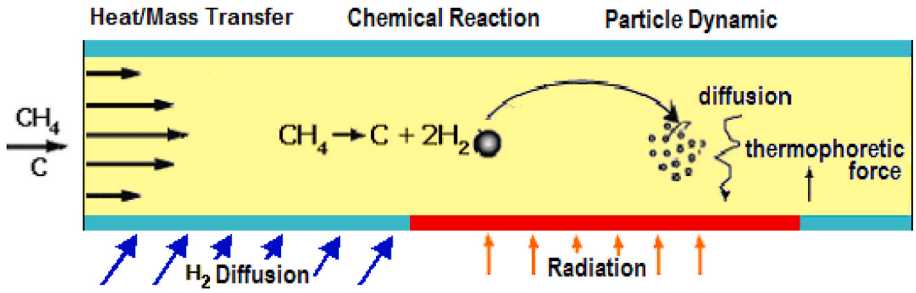


Fig. 2. Numerical model representation of aerosol flow reactor.

Table 1
Obtained equilibrium conversion of methane by Matowich [1,5].

T (K)	1533	1644	1755	1866	1955	2144
M_{CH4} (gr/s)						
0,304	0,86	0,94	0,915	0,94	0,97	1
0,608	0,74	0,79	0,83	0,88	0,94	1
0,912	0,66	0,72	0,78	0,845	0,925	1
1216	0,6	0,68	0,745	0,82	0,91	1
1,52	0,54	0,63	0,705	0,79	0,895	1

Table 2
Reynolds numbers with respect to Methane Feed Rate.

Methane Feed Rate (g/s)	Velocity (m/s)	Reynolds Number
0.304	0.15	360
0.608	0.30	720
0.912	0.45	1080
1.216	0.60	1440
1.520	0.75	1800

u = average gas velocity (m/s)
D = reactor diameter (m)
μ = dynamic viscosity of methane (Pa·s)

For the reactor dimensions used in this study (D = 0.076″ m"), methane feed rates of 0.304–1.52 g/s correspond to average velocities in the range of 0.15–0.75 m/s. Assuming a gas density of 0.25 kg/m^3 at 2000 K and a viscosity of 3.5 × 10^{-5} Pa s, the Reynolds numbers were calculated as follows.

These values remain below the typical transition threshold of Re ≈ 2300 for tubular reactors, confirming that laminar flow assumptions are valid under the studied operating conditions (see Table 2)

However, local turbulence can occur at high temperatures and higher flow rates, particularly in areas with strong particle-radiation interactions. Specifically, turbulence can accelerate methane conversion by enhancing convective heat transfer and species mixing. While the laminar assumption remains a reasonable approach for the current reactor configuration, it may be appropriate for future studies to incorporate turbulence models (e.g., RANS or LES) into the CFD framework to further validate prediction accuracy under solar-powered conditions.

The numerical model developed in this work has proven to be highly effective in defining the relevant process parameters and chemical kinetics associated with methane decomposition. By solving the governing equations within the FLUENT 6.0.12 environment, the model enables detailed analysis of flow behavior, reaction rates, and conversion distributions. These equations provide the mathematical foundation for capturing the coupled phenomena of fluid dynamics and chemical kinetics within the reactor environment. This integrated approach facilitates a deeper understanding of the decomposition process and supports the optimization of reactor design and operating conditions.

The governing equations applied in the simulations are presented in the following section, providing the mathematical basis for the CFD model and ensuring transparency in the methodology adopted [9].

6.1. Mathematical formulation and governing equations

The governing equations applied in this study are formulated for laminar flow fields within the aerosol reactor tube. These equations include the momentum equations incorporating the stress tensor, the continuity equation and the energy equation. The energy equation can be formulated in terms of the total energy (E), which is defined as the sum of internal energy and kinetic energy. The sensible enthalpy (h) is referenced to a standard temperature of 298.15 K, ensuring consistency in thermodynamic calculations.

The computational model for the laminar fields of flow in the aerosol reactor tube can be expresed on the following set of governing equations:

The conservation of mass is expressed as

$$\frac{\partial \rho}{\partial t}+\frac{\partial}{\partial x_i}(\rho u_i)=S_m \tag{6}$$

Momentum conservation is described by the Navier–Stokes equations as follows:

$$\frac{\partial}{\partial t}(\rho u_i)+\frac{\partial}{\partial x_j}\left(\rho u_i u_j\right)=-\frac{\partial p}{\partial x_i}+\frac{\partial \tau_{ij}}{\partial x_j}+\rho g_i+F_i \tag{7}$$

where the strees tensor at momentum equation is described as:

$$\tau_{ij}=\left[\mu\left(\frac{\partial u_i}{\partial x_j}+\frac{\partial u_j}{\partial x_i}\right)\right]-\frac{2}{3}\mu\frac{\partial u_l}{\partial x_l}\delta_{ij} \tag{8}$$

The energy equation accounts for conduction, convection, radiation, and chemical reaction heat effects can be formulated as follows

$$\frac{\partial}{\partial t}(\rho E)+\frac{\partial}{\partial x_i}\left(u_i(\rho E+p)\right)=\frac{\partial}{\partial x_i}\left(k_{eff}\frac{\partial T}{\partial x_i}-\sum_j h_{j'}J_{j'}+u_j\left(\tau_{ij}\right)_{eff}\right)+S_h \tag{9}$$

where total energy E can be formulated as follows:

$$E=h-\frac{p}{\rho}+\frac{u_i^2}{2} \tag{10}$$

Energy Source term, S_h in Eq. (4) includes the energy source due to chemical reaction:

$$S_{h,ixn}=-\sum_j\left(\frac{h_j^0}{M_j}+\int_{T_{ref,j}}^{T}c_{p,j}dT\right)R_j \tag{4}$$

Where R_j is the mass of the species of reactants and products and h_j^0 is enthalpy formation of species j.

Sensible enthalpy h at those equations can be formulated as

$$h=\sum_j m_j h_j \tag{5a}$$

and also elements of enthalpy can be ahown as:

$$h_j = \int_{T_{ref}}^{T} c_{pj} dT \tag{5b}$$

where T_{ref} is 298.15K.

Enthalpy transport resulting from species diffusion is accounted for in both the continuity and energy equations. as this following term is a requisite component of the energy equation:

$$\nabla \cdot \left(\sum_j h_j \vec{J}_j \right) \tag{11}$$

The conservation equations for chemical species are resolved to determine the local mass fraction of each species, ρm_i via the convection-diffusion equation for the ith species. The term R_i represents the net mass rate of production or consumption of species i resulting from chemical reactions, while Si denotes the additional source term defined below.

$$\frac{\partial}{\partial t}(\rho m_i) + \frac{\partial}{\partial x_i}(\rho u_i m_i) = -\frac{\partial}{\partial x_i} J_i + R_i + S_i \tag{12}$$

This source term accounts for hydrogen diffusion originating from the wall boundaries, as well as species production driven by decomposition reaction kinetics.

6.2. Source terms definition

The model resolves species transport by considering mass diffusion among the mixture components and the net volumetric rate of species production/consumption due to chemical reactions occurring throughout the tube reactor. Hydrogen is injected via a constant mass flux applied uniformly across the entire tube wall surface. The purpose of this injection is explicitly to inhibit particle deposition. The precise definitions of the mass diffusion and species conversion terms are detailed in the subsequent sections.

6.2.1. Mass diffusion in laminar flows

In the formulation of the species transport equations, the term J_i denotes the diffusion flux associated with species (i). This flux originates from concentration gradients within the mixture and represents the net movement of species driven by molecular diffusion. In the default treatment adopted by Fluent, the dilute approximation is applied. This approximation is particularly effective for multicomponent reacting flows in which the species of interest are present at relatively low concentrations compared to the bulk mixture, thereby reducing computational complexity while maintaining sufficient accuracy for engineering Analysis.

The diffusion flux can be expressed as follows in a simplified form that directly relates the gradient of the species mass fraction to its transport behavior:

$$J_{i',i} = -\rho D_{i',m} \frac{\partial m_{i'}}{\partial x_i} \tag{13}$$

6.2.2. Mathematical formulation of Gas-Phase Reaction Mechanism

Gas-Phase Reaction Mechanism can be formulated as follows:

$$\sum_{i=1}^{N_g} \nu'_{ik} X_i \rightarrow \sum_{i=1}^{N_g} \nu''_{ik} X_i \ (\mathrm{k} = 1 \ldots\ldots\ldots \mathrm{K_g}) \tag{14}$$

The chemical reaction mechanism considered in this study involves a total of K_g elementary reactions occurring in the gas phase. For each chemical species *i*, the net source term due to reaction R_i is evaluated as the cumulative contribution of all Arrhenius-based reaction rates across the N_R reactions in which the species participates. This formulation ensures that the production and consumption of species are accurately represented within the reactor environment.

$$R_{i'} = M_{i'} \sum_{k=1}^{N_R} \overset{\Lambda}{R} \tag{15}$$

The laminar finite-rate model implemented in the CFD framework is employed to compute the chemical source terms. In this model, the reaction rates are determined using Arrhenius-type expressions, which provide a temperature-dependent description of chemical kinetics. Reactions are assumed to occur within the continuous phase, involving interactions among continuous-phase species.

For the N^{th} reaction, the general form can be expressed as a stoichiometric relationship between reactants and products as follows:

$$\overset{\Lambda}{R} = \Gamma \left(\nu''_{i',k} - \nu'_{i',k} \right) \left(k_{f,k} \prod_{j'=1}^{N} \left[C_{j'} \right]^{\eta'_{j',k}} - k_{b,k} \prod_{j'=1}^{N} \left[C_{j'} \right]^{\eta''_{j',k}} \right) \tag{16}$$

The Arrhenius expression is employed to compute the forward rate constant, $k_{f,r}$, for reaction r:

$$k_{f,k} = A_k T^{\beta_k} \exp(-E_k / RT) \tag{17}$$

6.3. Radiative heat transfer equation

Considering the very high reaction temperatures and the nature of the carbon particle-loaded environment within the reactor, it appears that thermal radiation may be a dominant heat transfer mechanism. Consequently, the effect of radiative heat transfer must be incorporated into the numerical calculation model.

The governing equation for this process is the Radiative Transfer Equation (RTE), which describes the energy transport in an absorbing, emitting, and scattering medium. The RTE at position r in the direction s can be expressed as follows:

$$\frac{dI(r,s)}{ds} + (a + a_p + \sigma_s) I(r,s) = an^2 \frac{\sigma T^4}{\pi} + E_p + \frac{\sigma_s}{4\pi} \int_0^{4\pi} I(r,s') \Phi(s.s') d\Omega' \tag{18}$$

$(a + \sigma_s)s$ is the optical thickness or opacity of the medium. When considering radiation in semi-transparent media, the refractive index n becomes significant. In the discrete coordinate (DO) radiation heat transfer model, the radiation transfer equation (RTE) is solved using a finite number of discrete solid angles defined in the spherical Cartesian coordinate system, associated with the constant vector s in the (x; y) direction. The DO model allows us to include the effect of a discrete second particle phase on radiation heat transfer and to capture the contribution of the particle phase in the RTE.

Carbon particle optical properties were obtained from published datasets on soot and pyrolytic carbon. The spectral absorption coefficient value and scattering coefficient values have been taken as 120–150 m^{-1} 30–40 m^{-1} respectively. Emissivity values of 0.93 was used for the carbon particles, consistent with typical values for carbon black at high temperatures, as referenced in standard literature on radiative properties of particulates. The refractive index n = 1.55 was assumed constant across 300–1800K. Temperature dependence was incorporated by adjusting absorption and emissivity with particle size and thermal conditions. The DO radiation model was configured with 4 × 4 angular discretization, convergence tolerance of 1×10^{-3}, and gray wall boundary conditions with $\varepsilon = 0.9$. These settings ensure accurate resolution of radiation–particle interactions in the reactor.

6.4. The other effects and correction equations

The reacting flow mechanism is able to include thermophoresis and lifting effects, to be taken into consideration to obtain the most sensible model. For this reason, thermophoresis and lifting effects are defined optionally, and these are added to solving equation systems. Flowing includes two phase which consist of gas (methane-hydrogen) and solid

(carbon particle). During reacting flow, interaction of between two phases occurs. Therefore, it must be added correction to the governing equations.

6.4.1. Thermophoretic force term

Thermophoretic force and lift effect were also added general computing algorithm, and continous phase and discrete phase were combined to obtain actual flow mechanism. $D_{T,p}$ is thermophoretic constant. Thermophoresis effect formulation is

$$F_x = -D_{T,p}\frac{1}{m_p T}\frac{\partial T}{\partial x} \tag{19}$$

6.4.2. Lift effect

When flowing and converting gas mixture, lift effect also occurs in the tube. The lift effect formulation is used from Saffman formulation defined following equation [[15]].

$$\vec{F} = \frac{2K\nu^{1/2}\rho d_{ij}}{\rho_p d_p (d_{lk} d_{kl})^{1/4}}\left(\vec{v} - \vec{v}_p\right) \tag{20}$$

6.4.3. Discrete phase correction

A momentum and heat transfer interaction occur between continuous (gas) phase and discrete (particle) phase. Therefore, these terms must be integreted and make harmonious into general governing equations.

Momentum transformation equation

$$F = \sum\left(\frac{18\mu C_D Re}{\rho_p D_p^2 . 24_{p_{dig}}}()\overset{*}{m}_p\right) \tag{21}$$

Heat transformation equation

$$Q = \left[\frac{m_p}{m_{po}}c_p \Delta T_p + \frac{\Delta m_p}{m_{po}}\left(-h_{fg} + h_{ayr} + \int_{T_{ref}}^{T_p} c_{p,i}dT\right)\right]\overset{*}{m}_{po} \tag{22}$$

6.5. Boundary conditions

The boundary conditions required for our mathematical model in the simulation were defined as necessary and appropriate using the Fluent code. The reaction structure within the tube reactor was described by two-dimensional cylindrical geometry using conservation equations. The axial directions in the conservation equations specified by (1) - (6) were converted to Cartesian (x, y) coordinates, where x and y are independent variables. The methane and carbon mixed flow is assumed to be proportionally fed through the reactor inlet cross-section. This mixed flow enters the tube reactor calculation domain (x = 0 cm) with initial conditions of velocity, composition, and temperature determined through the inlet cross-section (y = 0). In all simulations at the inlet boundary, the axial velocity u and the vertical velocity uy = 0 profile at the boundary were used. The velocities for the boundary conditions at the tube wall were set to zero. The mass ratio values for the inlet conditions were taken from Table 1, and the methane inlet temperature was assumed to be 300 K and the pressure was 1 bar.

The outlet is defined as a pressure outlet boundary condition in ANSYS Fluent. This choice allows specifying the static pressure at the outlet and ensures numerical stability. The expression "body temperature = wall temperature" is used to avoid non-physical gradients at the boundary and to indicate that the return temperature is set equal to the wall temperature. Temperature gradients are resolved by the solver up to the outlet plane. Convective heat transfer is allowed to develop naturally, and the outlet condition ensures that the energy equation continues smoothly.

At the reactor exit (*x=0,914 ve y=(<0,d>)*), an outlet boundary is applied. Outlet flow conditions is defined as assuming body temperature as property of wall temperature. Particles for discrete condition type is assumed to escape type and internal emissivity value is 1. Outlet velocity and pressure are not defined. Flow outlets the computational domain (*x* = 0.914 cm) from over the cross section of inlet (y = <0-d>) at an unknown velocity, composition, and temperature.

Reactor wall is assumed as black body that irradite the mixture by using all of the energy into tube. Its internal emissivity = 1 and external emissivity = 0 for wall boundary condition. Particles is defined that have reflecting charecteristics on the wall for discrete movement condition. Convective heat transfer values is derived from Roberts formulation for each flow rate and temperatures [2]. There is hydrogen gas (0,188 gr/s) injection from porous wall into through the tube. This mass source is defined for wall BCs. Wall temperature is used from Table .1.

Carbon particles inlet values and conditions are defined at different panel in the programme. The diameter value of carbon particle is 5.10^{-5} m, particles distrubition is assumed to be uniform and carbon flow rate is constant.

7. Numerical simulation results and discussions

The computational investigation was based on a numerical model encompassing the conservation laws for mass flow, energy conversion, reaction kinetics, radiative heat transfer, and the discrete phase. The geometry was defined as a two-dimensional horizontal rectangular reactor, with the computational mesh generated using the GAMBIT software package. The modeling approach was developed to achieve the most accurate and optimized solution.

The simulations were performed utilizing the ANSYS_FLUENT_CFD software. This code employs a control volume-based finite difference scheme to solve the fundamental conservation laws. A key aspect of the solution strategy is the simultaneous calculation of thermophysical properties (viscosity, specific heat, thermal conductivity, absorption rate, and species diffusion coefficients), which are dynamically adjusted based on the local temperature and composition of the mixture. Model parameters (as listed in Table 1) were selected to provide the closest comparison to the experimental work of Matovich and the simulations conducted by Dahl and colleagues. The detailed methodology for the 2D simulations and associated numerical considerations are addressed elsewhere.

The numerical model facilitates the analysis of flow dynamics, energy transfer, reactive flow interactions, and key flow features, with results visualized as two-dimensional graphics. The reacting mixture is composed of CH_4, H_2 and solid carbon particles C(s), all utilizing properties available within the FLUENT database. Modeling radiative heat transfer in reactive flow environments presents a challenge, as the continually changing species composition leads to dynamic variations in radiative properties. Therefore, a careful selection of the most appropriate radiation model is necessary. The Discrete Ordinates (DO) Model was selected for implementation due to its sound theoretical basis and its ability to provide accurate and appropriate predictions of the radiative flux.

Aerosol tube reactor wall temperature and gas flow rates were selected to ensure reliability and provide a direct basis for comparison with the benchmark values established by Matovich and the subsequent simulations conducted by Dahl. Matovich's study represents the only available experimental data collected in a high-temperature aerosol reactor, which served as the foundation for the secondary validation values obtained by Dahl.

The parametric study investigated reactor wall temperatures ranging from 1533 K to 2144 K, while gas flow rates were maintained within the specified range of 0.304 g/s to 1.52 g/s. The resulting simulation data are detailed in the subsequent paragraphs.

The resulting conversion rates, based on flow rates for five distinct wall temperatures, are illustrated in Fig. 3. The sensitivity of methane decomposition conversion decreases as the flow rate increases across all temperatures investigated. Consequently, achieving maximum

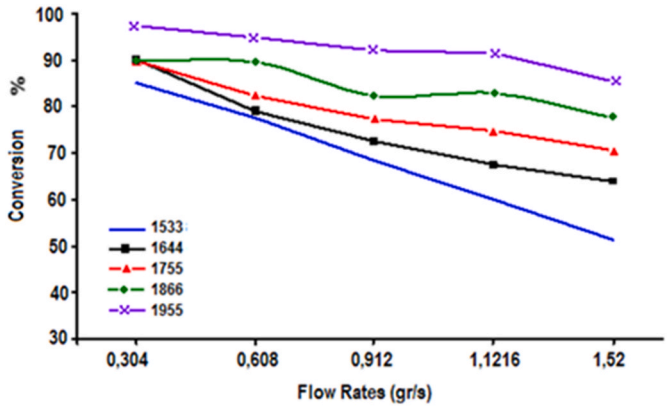


Fig. 3. Conversion values for different mass flow rates and different wall temperatures.

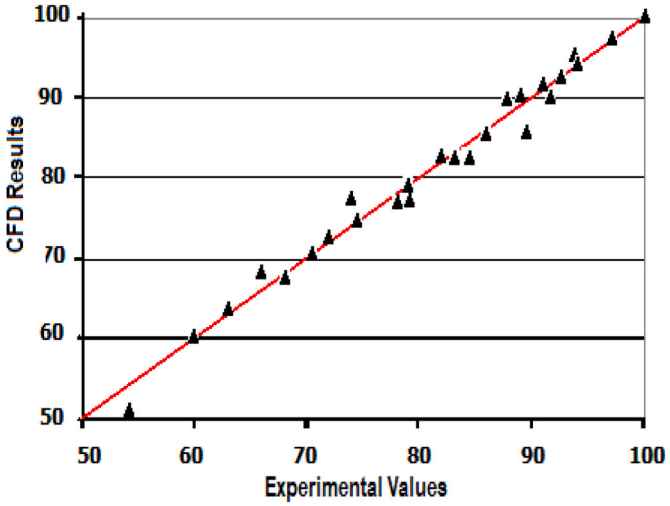


Fig. 4. Comparison of Obtained Results with Experimental Data. This figure presents a scatter plot comparing calculated values with experimental data. The data points cluster closely around the diagonal line, indicating strong agreement between simulation and experiment across the 30 data points analyzed.

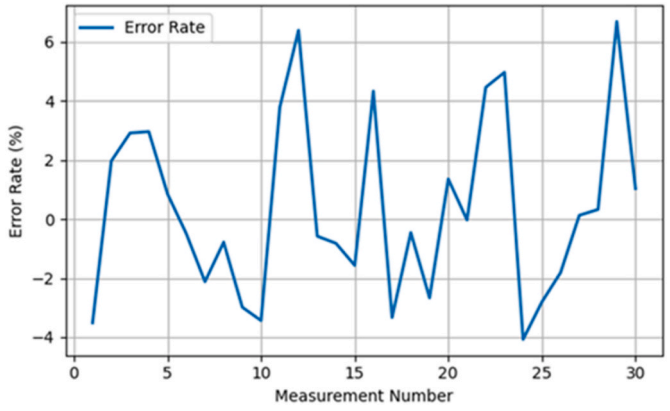


Fig. 5. Distribution of Error Rates. This figure shows the fluctuation of error rates (%) across different measurement indices. The values oscillate between +6% and −6%, indicating variability in experimental or simulation accuracy.

conversion requires maintaining high reactor temperatures while operating at optimized gas flow rates.A further critical consequence is the observed decrease in heat transfer effectiveness per unit of flow as the flow rate increases.

Reactor efficiency specifically denotes the thermochemical conversion efficiency of the system. It measures how successfully the reactor transforms incoming concentrated solar energy into chemical energy, which is stored in the hydrogen and solid carbon produced via methane decomposition. In this context, reactor efficiency is quantified as:

$$\eta = \frac{\text{Chemical energy contained in the output products}}{\text{Incident solar power supplied to the reactor}} \tag{23}$$

Operationally, it is the portion of the solar power entering the reactor aperture that is effectively used to drive the endothermic methane cracking reaction:

$$\eta_{th} = \frac{\dot{n}_{CH_4,conv} \times \Delta H^{\circ}_{rxn}}{\dot{Q}_{solar}} \tag{24}$$

Where:

$\dot{n}_{CH_4,conv}$ represents the molar flow rate of methane that undergoes conversion.

ΔH^{o}_{rxn} is the standard reaction enthalpy for $CH_4 \rightarrow C + 2H_2$.

$\dot{Q}_{solar}$ is the solar power absorbed by the reactor

This efficiency evaluates the overall performance of the aerosol-type solar reactor. It combines the effectiveness of the capturing solar radiation with the chemical conversion performance inside the reaction tube. Reactor efficiency is fundamentally a solar-to-chemical energy conversion efficiency. It assesses how well the integrated reactor system comprising a solar receiver and a aerosol reactor transforms concentrated solar heat into chemical energy via methane pyrolysis.

Fig. 6 illustrates the axial progression of molar methane conversion rates along the reactor length, parameterized by six different wall temperatures and five distinct gas flow rates.

At the lowest wall temperature (T = 1533 K), the onset of methane decomposition is significantly delayed, occurring between 3 cm and 20 cm from the reactor inlet. This decomposition onset length is highest at the maximum flow rate of 1.52 g/s and lowest at the minimum flow rate of 0.304 g/s. This result indicates that the supplied thermal energy is insufficient to fully meet the reaction activation energy, and that the heat transfer rate becomes limiting as the gas flow rate increases.

Similarly, decomposition initiates earlier, between approximately 0 cm and 20 cm, at T = 1644 K. Furthermore, the decomposition characteristics and spatial expansion are quite close to those observed at 1533 K.

For the higher wall temperatures studied, methane decomposition initiates near the reactor inlet (L = 0 cm). The conversion curve inclination (the rate of change of conversion per unit length) rises sharply with increasing wall temperature, signifying a substantial increase in the chemical reaction rate. Conversely, for a fixed wall temperature, this inclination consistently decreases as the flow rate increases, reflecting the reduction in residence time available for reaction (Fig. 7).

Fig. 8 illustrates the relationship between methane conversion rates and wall temperatures, parameterized across three distinct, uniformly spaced flow rates (0.304, 0.912 and 1.52 g/s).

A dimensionless formulation was established to characterize heat transfer within an aerosol flow reactor measuring 0.076 m in diameter and 0.91 m in length, designed for methane decomposition into hydrogen and carbon black. The equations were solved to assess the sensitivity of three operating parameters: carbon particle size, particle feed molar flow rate, and reactor wall temperature. The analysis shows that nearly complete methane conversion requires wall temperatures close to 2100 K. Furthermore, effective heat transfer to the gas phase is promoted when carbon black particles with radii of 5 μm (surface area $\approx 3.1 \times 10^{-10}$ m^2) or smaller are introduced. The precise particle feed rate is less critical, provided it remains on the order of 0.01 mol/s. These operating conditions correspond to reactors with residence times of approximately 0.1 s.

This evidence strongly supports the conclusion that temperature is

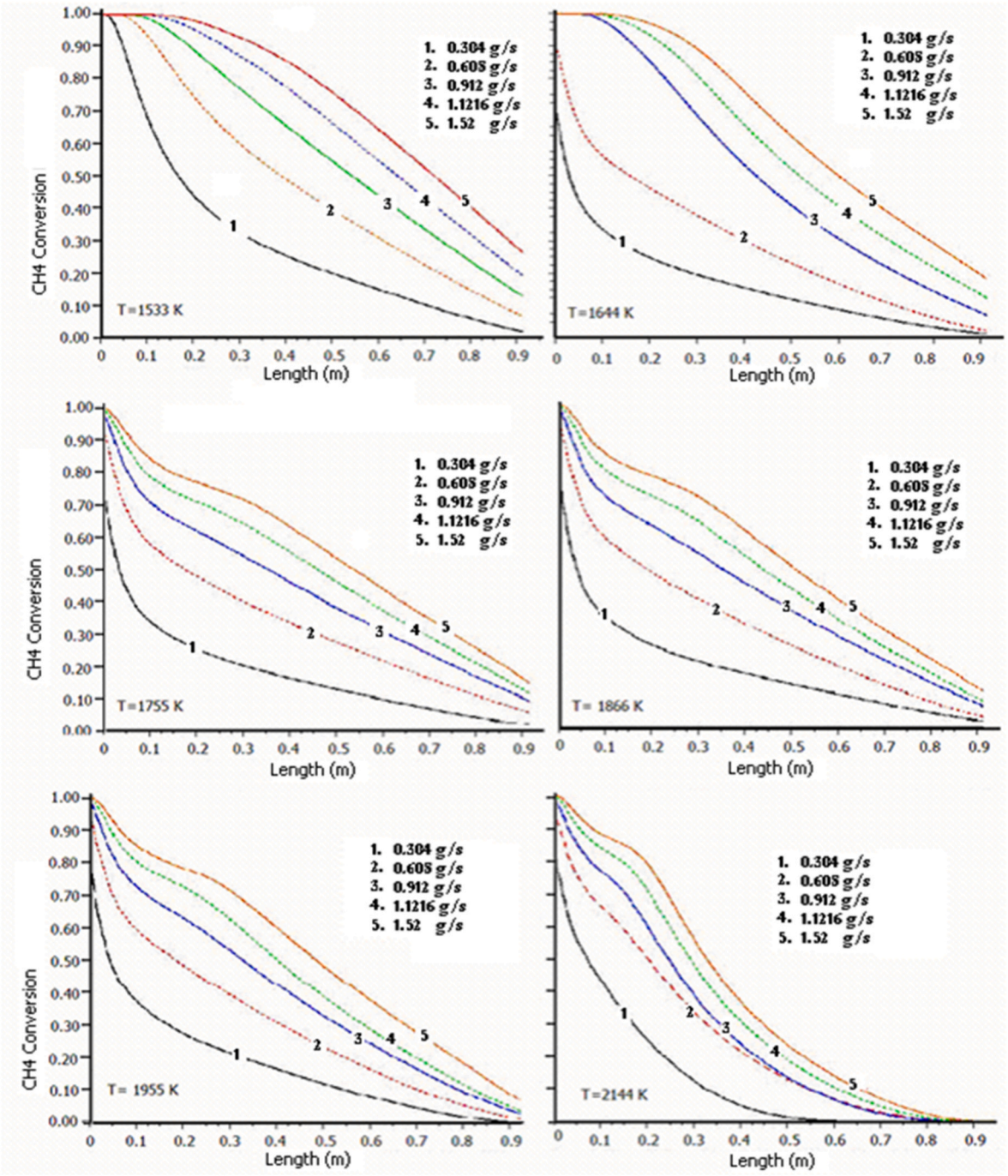


Fig. 6. Methane conversion values through tube for 6 temperature values and 5 flow rates.

the most significant governing factor dictating the methane decomposition mechanism within this reactor configuration.

Given the catalytic role of the solid carbon particles in the reaction, it is essential to characterize the thermal relationship between the particle phase and the gas phase. Fig. 6 presents a comparative plot of these phase temperatures along the reactor axis. The plot reveals that the particle temperature exceeds the gas phase temperature within the initial 20 cm of the reactor length. Downstream of this region, the two temperatures begin to converge, achieving near-stationary values toward the reactor exit. Carbon particle effect on decomposition can be clearly seen from this temperatures expanding, when comparing and analysing with the other figure solutions about decomposition expandings.

The conversion values were obtained by significantly narrowing the optimal kinetic data range reported in the studies of Wiemer and colleagues. The values used were an activation energy range of 200–211 kJ/mol and a reaction rate constant of 6–12 $\times$ 10^{11} s^{-1}. These narrowed values fall within the 200–230 kJ/mol range identified by Muradov, thus aligning well with all three studies. Additionally, a temperature range consistent with the decomposition mechanism reported in the literature was established. A comparison of the obtained results with experimental data is presented in Fig. 4. As seen, the results are quite close to each other. This comparison, conducted over 30 data points, yielded values that are more consistent with experimental data than those previously analyzed by Dahl and colleagues. The error analysis for the same data is provided in Fig. 5. According to this analysis, the error

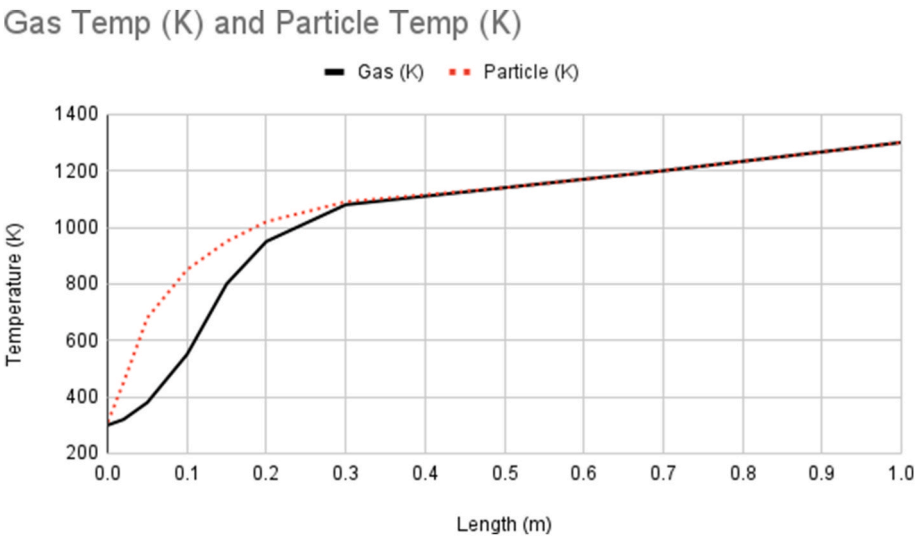


Fig. 7. Gas and particle temperature according to tube length (T_w = 1755 K,0.912 gr/s).

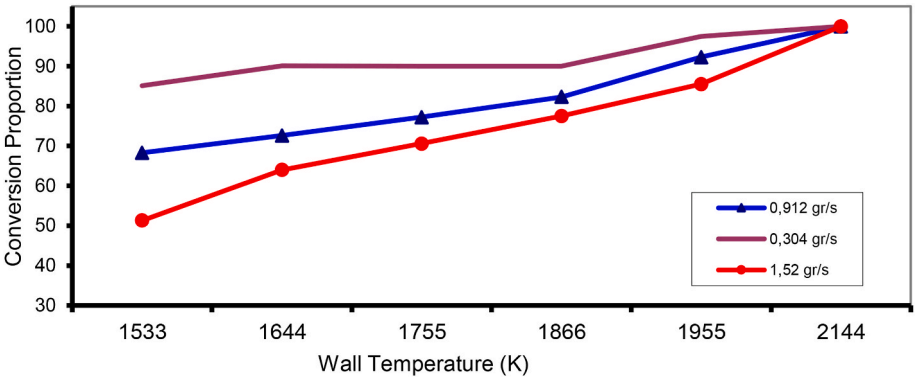


Fig. 8. Conversion values according to wall temperature for three flow).

range varies between −5% and +5%, with an average error rate of 5%. This value is acceptable for a heterogeneous reaction environment. At higher temperatures, the error rate decreases even further.

The most important solution direction of the model is shown in Fig. 2 because of reacting expanding in the reactor as differentally form the other studies. Extension of the methane decomposition through the reactor tube is indicated in this figure for 1533 K wall temperature at five different flow rates as two dimensional. It makes full distrubition of the species through the tube to be possible.

For example, it can be understood of inlet velocity effect on the beginning of the reaction and hydrogen diffusing that is towards inside of tube from wall on mechanism extension. Species distrubition through the tube is closest connected to flow rates. Decomposition occurs annular through the tube and resembles to gas firing inside of the tunnel as natural gas and hydrogen.

Solution parameters of the numerical model on methane decomposition are indicated as far as here.

Another respect of this study is relation to the former study's results. Obtaining values from the model solution are compared with Matowich study's data. This is shown in Fig. 8 that contains comparative values that are obtained numerical model with Matowich study's data. Conversion values are very closest to data that is given at Table .1. These values were obtained by getting closer kinetics parameters and constants that are used in wide range.

To ensure the reliability of the kinetic model, the activation energy was constrained within the range of 200-211 kJ/kmol and the reaction constant factor was fixed between 6 and 12 $\times$ 10^{11} s^{-1} for all simulations.

The selected activation energy range exhibits strong agreement with the benchmark data reported by Muradov, which specified values between 200_230 kJ/kmol. In this respect, the obtained kinetic parameters are harmonious and consistent with the data derived from three separate external experimental studies.

8. Conclusion

The CFD simulation model of the methane decomposition mechanism in this study includes detailed flow-thermal-chemical reactions, discrete phase flow, and associated complex mathematical operations. This numerical model allows us to analyze the effects of various parameters that may influence the reaction mechanism in an aerosol tube flow from various engineering perspectives, including chemical, mechanical, and reaction kinetics.

Our application of CFD, linked to various engineering disciplines, can provide useful analyses for reaction problems in such flows. Such simulations will enable us to create newer designs and develop applicable, functional reactor models. Methane decomposition and kinetic analysis is an important field encompassing many important and comprehensive parameters. One of these parameters is activation energy, which can vary depending on many variables such as catalyst properties, particle geometry, microchemical structure, and so on. Therefore, there is no fixed value for chemical kinetic properties, and understanding the chemical reaction kinetics for such heterogeneous reactions is quite challenging. Another conclusion from this study is that this modeling allows for the understanding and identification of

sensitivity characteristics for parameters by examining various application aspects in green hydrogen engineering. High-temperature thermal cracking (MTD) of methane in an aerosol flow reactor offers a technologically advanced and economically promising method for CO_2-free hydrogen production. The designs developed through these simulations provide a clearer understanding of the fundamental challenges inherent in MTD processing the activated carbon and hydrogen.

This modeling study will enable more precise process control capabilities for AFR. This will enable the production of high-purity hydrogen, as well as the design of high-value activated black carbon production, and the transformation of a potential waste into a critical economic driver.

While some challenges remain in catalyst control and scaling, research and development studies similar to our CFD analysis study demonstrate that the MTD-AFR process can be considered a serious contender for the future of clean and green hydrogen production in upgrade applications using biomethane and natural gas.

The economic viability of methane decomposition is significantly influenced by the marketability of its carbon byproduct. As Riley et al. [31] suggest, if all the carbon generated during the process could be sold at 0.82 EUR/kg, the cost of hydrogen production could drop from 2.68 EUR/kg to zero. According to the International Energy Agency (IEA), global hydrogen production in 2019 was approximately 115 million tons. Given the stoichiometric relationship in methane pyrolysis, this would result in around 345 million tons of carbon—three times the mass of hydrogen produced. However, this figure far exceeds the current global annual demand for solid carbon, which is less than 20 million tons [30]. Consequently, large-scale implementation of methane cracking could oversaturate the carbon market. To support the transition to green hydrogen via methane pyrolysis, strategies for carbon sequestration or the development of new industrial applications for solid carbon are essential.

Moreover, the economic impact of carbon recovery depends on its form and quality, as different types of carbon command varying market prices. For instance, carbon black typically sells for 0.3–1.7 EUR/kg, while graphitic carbon can reach 8 EUR/kg, and carbon fibers range from 20 to 94 EUR/kg [29]. Additionally, research indicates that higher dilution ratios during the process tend to produce larger carbon particles [28], which may further influence their commercial value and usability.

CRediT authorship contribution statement

İzzet Karabay: Writing – original draft. **İsmail Ekmekci:** Validation, Supervision, Conceptualization.

Declaration of competing interest

The authors declare that they have no known competing financial interests or personal relationships that could have appeared to influence the work reported in this paper.

References

[1] Dahl JK, Barocas, Clough DE, Weimer AV. Intrinsic kinetics for rapid decomposition of methane in an aerosol reactor. Int J Hydrogen Energy 2002;27:377–86.

[2] Weimer,A.V., DahlJ., and BuechlerK., “Thermal dissocation of methane using a solar coupled aerosol flow reactor” , Proceeding of the 2001 DOE hydrogen program review, NREL/CP-570-30535.

[3] Snoeck JW, Froment GF, Fowlest M. Kinetic study of the filament formation by methane cracking on a nickel catalyst. J Catal 1997;169:250–62.

[4] Deutschmann O, Schmith LD. Two dimensional modeling of partial oxidation of methane in a short contact time reactor. AIChE J 1998;44:2465–76.

[5] Matowich E. Thagard tecnology company. United States patent #4095974. 1978.

[6] Hirsch D, Steinfeld A. Solar hydrogen production by thermal decomposition of natural gas using a vortex-flow reactor. Int J Hydrogen Energy 2004;29(Issue 1):47–55.

[7] Trommer D, Hirsch D, Steinfeld A. Kinetic investigation of the thermal decomposition of CH_4 by direct irradiation of a vortex-flow laden with carbon particles. Int J Hydrogen Energy 2004;29(Issue 6):627–33.

[8] Stephane A, Flamant G. Solar hydrogen production from the thermal splitting of methane in a high temperature solar chemical reactor. Sol Energy 2005;80 (Issue.10):1321–32. https://doi.org/10.1016/j.solener.2005.11.004.

[9] Mianowski A, Szul M, Radko T, Sobolewski A, Iluk T. Reciever/reactor concepts for thermochemical transport of solar energy. Energies 2024;17(Issue.19):1–33. https://doi.org/10.3390/en17195007.

[10] Moghaddam, AL., Hejazi, S., Fattahi, M. Kibria, MG., Thomson, MJ., Aleisa, R., Khan, MA., Methane pyrolysis for hydrogen production:navigating the path to a net zero future, Energy Environ Sci, v.18, Issue.6, pp.2747-2790, https://doi.org/10.1039/d4ee06191h,.

[11] Kim MH, Lee EK, Jun JH, Kong SJ, Han GY, Lee BK, Lee T, Yoon KJ. Hydrogen production by catalytic decomposition of methane over activated carbons: kinetic study. Int J Hydrogen Energy February 2004;29(2):187–93.

[12] Steinberg M, Cheng HC. Modern and prospective technologies for hydrogen production from fossil fuels. Int J Hydrogen Energy 1989;14:797–820.

[13] Muradov N. Hydrogen via methane decomposition: an application for decarbonization of fossil fuels. Int J Hydrogen Energy 2001;26:1165–75.

[14] Muradov N. Catalysis of methane over elemental carbon. Catalysis Comunication 2001;2:89–94.

[15] Saffman PG. The lift on a small sphere in a slow shear flow. J Fluid Mech 1965;22:385–400.

[16] Chan SH, Wang HM. Thermodynamic analysis of natural-gas fuel processing for fuel cell applications. Int J Hydrogen Energy 2000;25:441–9.

[17] Rozenman T. Energy transport with an integrated direct solar reactor. J Sol Energy Eng 1990;112:140–5.

[18] Diver RB. Reciever/reactor concepts for thermochemical transport of solar energy. J Sol Energy Eng 1987;109:199–204.

[19] FLUENT_6.1_User's Guide. Fluent Inc.Centerra resource park 10 cavendish court Lebanon, NH 03766. February 2003.

[20] Gruse WA, Donald R. The chemical technology of petroleum. Newyork: Stevens Mc.Graw-Hill; 1942. p. 356.

[21] Muradov N, Smith F, Huang C, T-Raissi A. Autothermal catalytic pyrolysis of methane as a new route to hydrogen production with reduced CO2 emissions. Catal Today 2006;116:281–8.

[22] Rodat S, Abanades S, Coulié J, Flamant G. Kinetic modelling of methane decomposition in a tubular solar reactor. Chem Eng J 2009;146:120–7.

[23] Keipi T, Tolvanen KES, Tolvanen H, Konttinen J. Thermo-catalytic decomposition of methane: the effect of reaction parameters on process design and the utilization possibilities of the produced carbon. Energy Convers Manag 2016;126:923–34.

[24] Abanades S, Flamant G. Experimental study and modeling of a high-temperature solar chemical reactor for hydrogen production from methane cracking. Int J Hydrog Energy 2007;32:1508–15.

[25] Sajid MU, Bicer Y. Thermodynamic assessment of chemical looping combustion and solar thermal methane cracking-based integrated system for green ammonia production. Therm Sci Eng Prog 2020;19:100588.

[26] Gonzalez-Aguilar J, Dème I, Fulcheri L, Flamant G, Gruenberger TM, Ravary B. Comparison of simple particle-radiation coupling models applied on a plasma black process. Plasma Chem Plasma Process 2004;24:603–23.

[27] Holmen A, Olsvik O, Rokstad OA. Pyrolysis of natural gas: chemistry and process concepts. Fuel Process Technol 1995;42:249–67.

[28] Abánades A, Ruiz E, Ferruelo EM, Hernández F, Cabanillas A, Martínez-Val JM, Rubio JA, López C, Gavela R, Barrera G, et al. Experimental analysis of direct thermal methane cracking. Int J Hydrog Energy 2011;36:12877–86.

[29] Dagle RA, Dagle V, Bearden MD, Holladay JD, Krause TR, Ahmed S. An overview of natural gas conversion technologies for Co-Production of hydrogen and value-added solid carbon products. WA, USA: Pacific Northwest National Lab: Richland; 2017.

[30] Muradov N, Veziroglu T. “Green” path from fossil-based to hydrogen economy: an overview of carbon-neutral technologies. Int J Hydrog Energy 2008;33:6804–39.

[31] Riley J, Atallah C, Siriwardane R, Stevens R. Technoeconomic analysis for hydrogen and carbon Co-Production via catalytic pyrolysis of methane. Int J Hydrog Energy 2021;46(39):20338–58. https://doi.org/10.1016/j.ijhydene.2021.03.151.